Computational Methods
for Shell and Spatial Structures
IASS-IACM 2000
M. Papadrakakis, A. Samartin and E. Oñate (Eds.)

STIFFENING METHOD FOR "SPRING-BACK" REFLECTORS

Lin Tze Tan and Sergio Pellegrino

Department of Engineering
University of Cambridge, Cambridge, UK
e-mail: pellegrino@eng.cam.ac.uk

Key words: Deployable Antenna, Shell Structure

Abstract. *The recently proposed concept of spring back reflectors has revolutionised the field of deployable antenna structures. The whole structure is made as a single piece from composite material, without any expensive and potentially unreliable joints, and it is simply folded elastically about a central axis, like a taco shell. Shape distortions occur during manufacturing and are difficult to correct due to the low stiffness of the structure. A stiffening method is proposed, that consists of a narrow skirt connected to the edge of reflector, with up to four radial cuts. It is shown that this system can increase the stiffness of a 5 m dish by a factor of 20 and the fundamental natural frequency by a factor of 7.4. The increase in the maximum stress level during packaging is minimal and the mass of the reflector increases by 16%.*

1 Introduction

The Hughes Space and Communications Company has revolutionised the field of deployable antenna structures by developing the so-called *Spring Back Antenna* [1, 2] shown schematically in Figure 1. This new concept consists of a thin-walled graphite mesh dish with an integral lattice of ribs and connecting elements, and with a stiffening edge beam along the rim. The whole structure is made as a single piece, from triaxial plies of carbon-fibre reinforced plastic (CFRP), without any expensive and potentially unreliable joints.

The folding concept is both simple and effective: since there are no joints or hinges, it is simply folded elastically about a central axis, like a taco shell, and is then stowed in the normally unused space in the nose cone of the rocket launcher. Once in orbit, the tie cables that hold the reflector in its packaged configuration are released, and the reflector deploys dynamically by releasing its stored elastic strain energy.

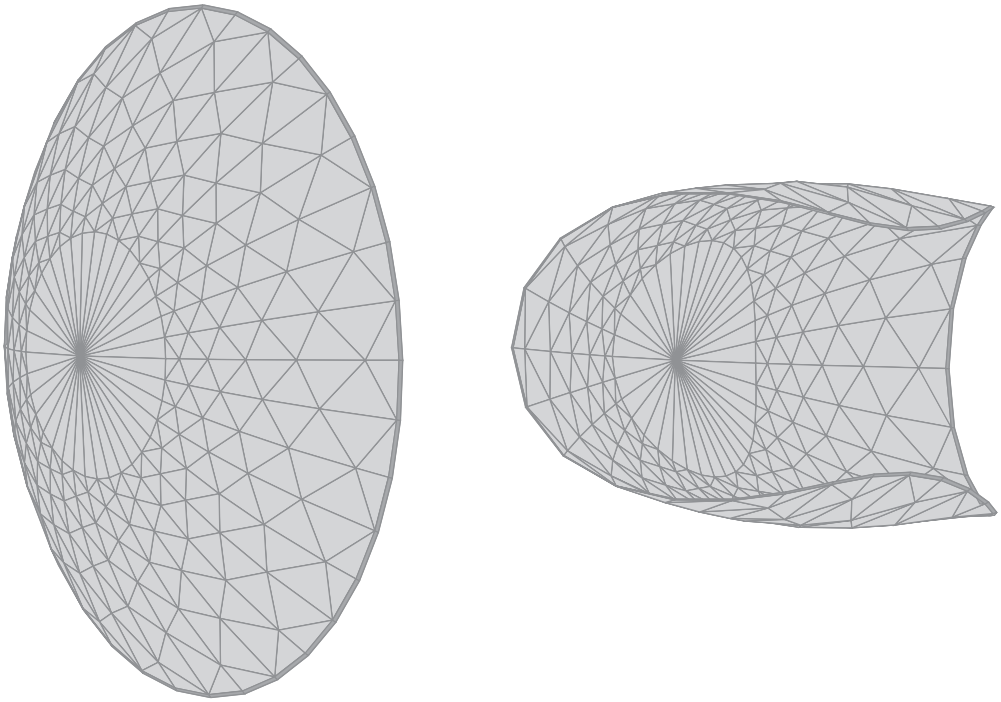

Figure 1: Schematic views of spring-back reflector, folded and deployed configurations.

Spring-back reflectors need to have low stiffness in order to be folded, but it is precisely their low stiffness that makes it difficult for them to achieve and retain a high shape accuracy. Furthermore, shape distortions that occur during the manufacturing of thin graphite structures —of the order $D/1000$ in the present case— make it even more difficult to meet the stringent shape accuracy requirements imposed on communications antennas. This is a significant problem, and potentially a severe limitation on the applicability of spring-back reflectors. Although the surface of the reflector can be adjusted with relatively simple mechanical devices, this defies the simplicity of

the concept and reduces the reliability of the complete system.

This paper proposes a modification of the original spring-back reflector concept, based on the idea of adding a thin-walled stiffening element around the edge of the dish. This element significantly increases the overall stiffness of the dish in the deployed configuration, and yet its configuration is such that the stiffened dish can still be folded elastically. The viability of this approach, which was demonstrated by means of simple physical models at the beginning of the present study, requires a good understanding of the folding properties of dishes in which stiffening elements are arranged in different ways. Simple physical models can give some useful insight, but a quantitative understanding of the effects of changing the various parameters of the stiffening element can be obtained only from a series of numerical simulations. Hence, results from an extensive set of finite-element simulations of the full non-linear behaviour of reflectors with different configurations are presented in the paper. Based on these results, some particular configurations that warrant further investigation are identified.

The layout of the paper is as follows. Section 2 presents the stiffening method that is proposed. Section 3 gives details of the finite-element simulation techniques that have been used in the present study. Section 4 presents an in-depth study of a small scale, simplified reflector structure, which serves to develops a qualitative understanding of the effects of varying several design parameters of the stiffening system. Based on this study, it is concluded that the system that works best has a narrow skirt, of width equal to about $1/20^{th}$ of the diameter of the reflector, with two or at most four cuts. Section 5 applies these results to the preliminary design of the stiffening system for a 5.0 m diameter spring-back reflector, and shows that a 125 mm wide skirt with two cuts provides a 20-fold stiffness increase and a 7.4-fold frequency increase, whereas a skirt with four cuts provides a 5-fold stiffness increase and a 1.6-fold frequency increase. A discussion of these results follows in Section 6, and the conclusions are summarised in Section 7.

2 Stiffening method

In general, the stiffer one makes a structure, the “harder” it becomes to fold it elastically. This intuitive statement can be formalised using an argument based on the total strain energy in the structure being equal to the work done by two equal and opposite forces that are applied to the structure in order to fold it. If the “stiffness” is increased the strain energy required to fold the structure by a given amount will increase proportionally. In general, the maximum strain and stress in the structure will also increase.

A spring-back reflector could be stiffened by increasing the stiffness of the edge rim or the ribs. However, increasing the thickness of these elements has the effect of making the maximum stress level in the folded reflector unacceptably high, while increasing their width is inefficient in terms of mass.

In general, an efficient way of increasing the stiffness of a structure is to prevent it from deforming in its lowest stiffness eigenmode. In the case of an “open cap” shell this eigenmode is the inextensional mode sketched in Figure 2(a). This eigenmode can be practically eliminated by

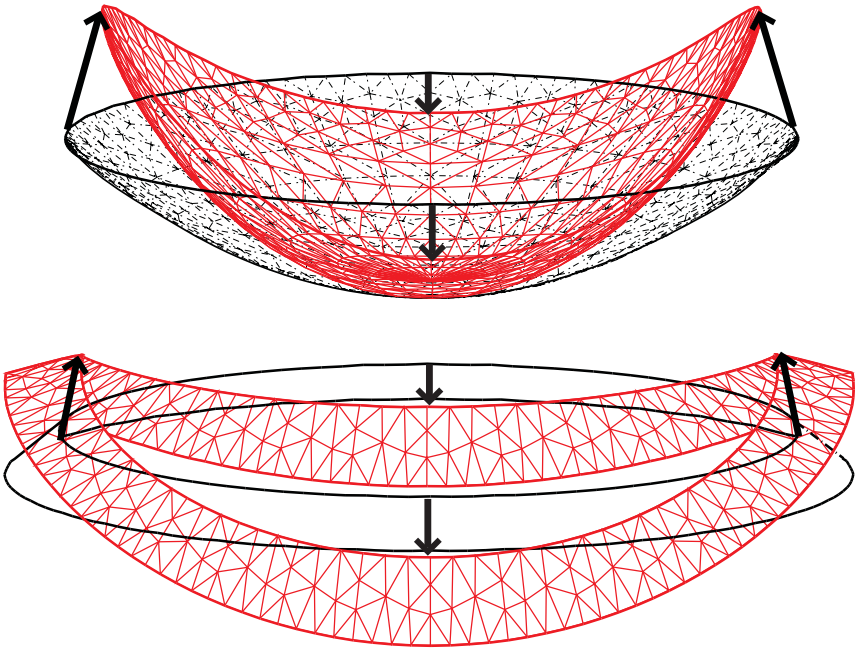

Figure 2: Lowest stiffness, incompatible eigenmodes of dish and skirt.

connecting the shell to a second shell whose lowest stiffness eigenmode is similar, but incompatible with that of the first shell. The second shell could be spherical or conical; the exact shape does not make much difference and hence, for simplicity a conical shape has been chosen, see Figure 2(b). This forms a *skirt* around the reflector whose width and angle to the edge of the reflector are design parameters to be decided.

The problem is that the addition of a continuous skirt around the reflector makes it so stiff that it can no longer be folded. However, by introducing a small number of radial cuts in the skirt one obtains a system whose stiffness can be tuned as required. A particular feature that is obtained in some cases is that the cuts allow the skirt to snap through while the reflector is being folded, which decreases the force required to fold the reflector. A potentially negative effect of introducing cuts in any structure, of course, is that they can result in high stress concentrations. However, these can be eliminated by controlling the stiffness distribution near the cuts and by designing out sharp edges. Finally, it should be noted that the idea of introducing cuts in a thin-walled reflector structure is not new: it was used in reference [3] to allow the formation of localised folds in the surface.

There are so many different ways of implementing these ideas that the only practical way forward is to examine the behaviour of some particular configurations of the stiffening system, in order to identify some viable solutions. This has been done for a particular system that is representative of a simplified $1/10^{\text{th}}$ scale model of a real spring-back antenna.

3 Modelling details

All simulations presented in this paper were made with ABAQUS [4] running on an HP C180 workstation. The meshes were generated with PATRAN [5] and the results were visualised with the ABAQUS post-processor.

The analysis is a non linear static analysis under displacement control, the moving boundary conditions being applied to two sets of nodes that are diametrically opposite on the rim. Initially, edge rotations, instead of translations, were applied. This appeared to work better at first but —once the mesh elements and run parameters had been optimised— it was found that edge rotations tend to produce localised deformation of the dish. Imposing a set of edge translations is the easiest and most reliable way of deforming the dish into the correct packaged shape.

The first structure that was analysed is a small-scale, highly simplified model of the reflector, with uniform thickness and material properties. A mesh of 6-node triangular thin shell elements (STRI65) was used at first, but convergence problems were encountered. A finer mesh of 3-node triangular elements (STRI35), with average density of 4000 elements/m^2, worked better but still produced occasional convergence problems. Finally, general 3-node shell elements (S3R) were used, and convergence was achieved throughout the time step. To keep the model small, it is possible to analyse only one quarter of the dish, with appropriate boundary conditions. This was done for the large dish with all the detailed features described in Section 5, but was unnecessary in the case of the dish of uniform thickness.

Depending on the width of the skirt, up to five rows of S3R elements were used to model the skirt. These formed a conical surface which was fully-connected to the rim of the reflector. The cuts in the skirt were modelled by not "equivalencing" the nodes on either side of the cuts; thus these nodes were not connected, although geometrically coincident.

The second structure that was analysed is the full-scale reflector. The continuous, uniform thickness shell was initially modelled with a mesh of thin-shell triangular elements (but see later), the 36 radial rib reinforcements were modelled with 3-node, rectangular section, standard formulation beam elements (B32), and the triangulation connecting the ribs with 2-node beam elements (B31). Finally, the rim reinforcement was modelled by 4-node quadrilateral shell elements (S4R5).

To set up all these features, each section of the antenna between triangulations was formed as a separate curved surface that conforms to the overall parabolic shape of the antenna. Due to the amount of detail required in the model and the large number of elements, only a quarter of the whole structure was modelled.

Again, thin shell elements gave convergence problems, but this time difficulties were still encountered with the same 3-node general shell elements that had worked well for the reflector of uniform thickness. However, reasonably robust convergence was achieved by increasing the iteration control parameters in ABAQUS as follows. The residual control from the default value, $\mathrm{R}_n^\alpha = 5 \times 10^{-3}$, to 5×10^{-2}; the solution correction control, C_n^α, was increased from 1×10^{-2} to 1×10^{-1}; the number of equilibrium iterations for the residual check, I_o, from 4 to 12; and the logarithmic rate of convergence check, I_R from 8 to 18.

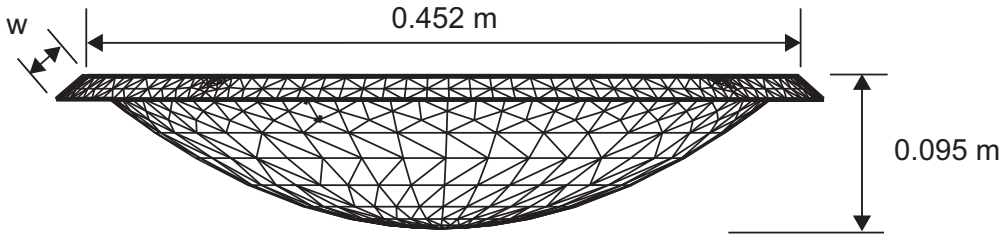

Figure 3: Dimensions of small reflector.

4 Small reflector of uniform thickness

The geometry and material properties of this reflector were defined on the basis of a physical model that had been used for some preliminary experiments. The dish has diameter $D = 0.452$ m, focal length $F = 0.134$ m ($F/D = 0.296$) and thicknesses $t = 1 - 4$ mm. Its overall shape, for a skirt width $w = 22$ mm, is shown in Figure 3; the angle of the skirt to the dish is approximately 100° (or 50° from the vertical). The whole structure is made from a low creep thermoplastic, called Vivak. This material is reasonably isotropic after vacuum forming; its elastic properties are: Young's Modulus $E = 2.05 \times 10^3$ N/mm^2 and Poisson's ratio $\nu = 0.3$.

Extensive simulations of this reflector were carried out, in order to determine how the stiffness of the reflector varies with the following properties:

- skirt width;
- number of cuts in the skirt;
- thickness of the reflector;
- position of the points which are pulled towards one another during folding.

The results of these simulations will be analysed by considering both the stiffness of the reflector, expressed in terms of its fundamental natural frequency of vibration, and the maximum stress in the packaged configuration, defined as the configuration in which the diameter length has been reduced by approximately 50%. The relationship between the force applied to the edge of the reflector and the corresponding displacement will also be examined.

The stress magnitudes that are considered in this section represent the highest Von Mises surface stress present in the dish after removing 3% of the most highly stressed nodes in the mesh. This approach is justified by the fact that the stress concentrations at the tip of each cut can be designed out at a later stage; in any case, this is the only way of getting a meaningful picture of the maximum stresses occurring in the dish.

Figure 5 shows the five different loading configurations that will be examined. It is worth noting that if one of the two forces that pull in the edges of the reflector is applied near a cut, the two pieces of skirt near that cut will overlap as the reflector is folded, whereas the cuts which

Analysis	No. cuts	t (mm)	w (mm)	σ_{max} (N/mm ^{2})
O1	-	2	0	19
A	2	2	86	129
B	4			68
C	2		43	71
D	4			54
E	2		22	51
F	4			38
G		1	86	37
H		4		125

Table 1: σ_{max} in packaged configuration, P at the cuts.

are located at 90° to the two forces will open out. Lastly, cuts located at 45° from the point of application of the forces will deform in shear.

4.1 Different configurations

Tables 1 and 2 show the results of investigations into several different dish configurations. The effect of varying the skirt width is clearly seen by comparing analyses A, C, and E: halving w results in a decrease of σ_{max} by 45% and halving it again causes a further reduction of 28%. Plotting these results, Figure 4(a), one finds that σ_{max} increases approximately linearly with w for the dish with two cuts. A similar trend is seen in the dish with four cuts, analyses B, D and F, but the rate of increase is much lower. This is because in the two-cut configurations the skirt provides a significant amount of additional stiffness, which acts against folding, whereas in the four-cut configurations the stiffness of the skirt plays a smaller role.

The effect of varying the (uniform) thickness of the reflector in a four-cut configuration with a rather wide skirt is seen by comparing analyses G, B and H, Figure 4(b). σ_{max} is proportional to t, which indicates that the highest curvature in the reflector remains essentially unchanged when t is increased, and in-plane stretching does not play a significant role.

From these results, it can be concluded that the best way of keeping σ_{max} low is to design reflectors with narrow skirt, four cuts, and with the smallest possible thickness.

Next, the effect of varying the skirt width and the number of cuts on the fundamental natural frequency of vibration of the reflector is investigated. The vibration mode of interest is the lowest stiffness eigenmode in the deployed configuration, see Figure 2; the frequency f of this mode has been calculated for the same configurations A-F analysed above, plus a reference configuration O2, with a continuous skirt. The results, listed in Table 2, show that

- the addition of the skirt increases the fundamental frequency f;
- wider skirts are less effective;

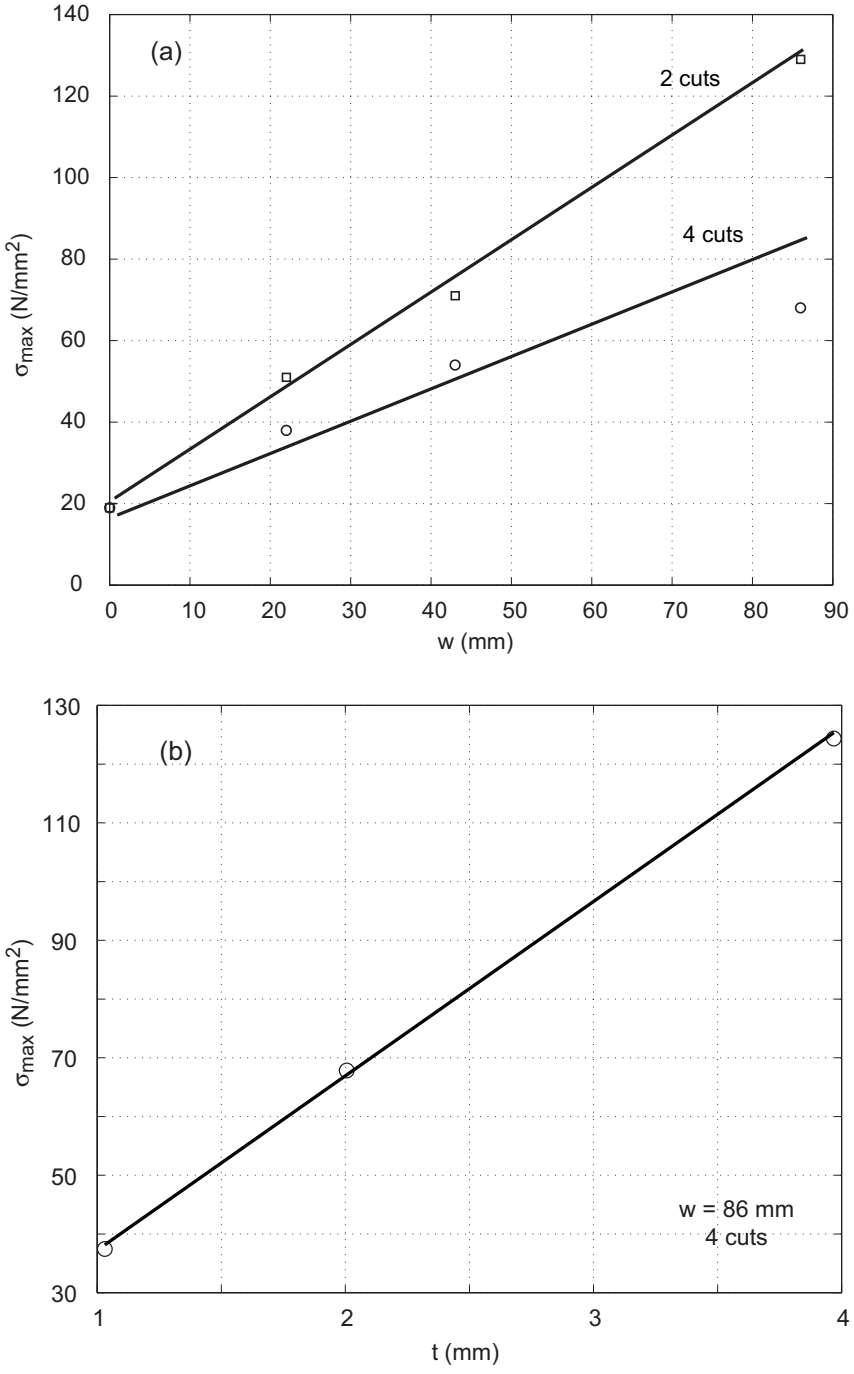

Figure 4: Variation of σ_{max} with w and t.

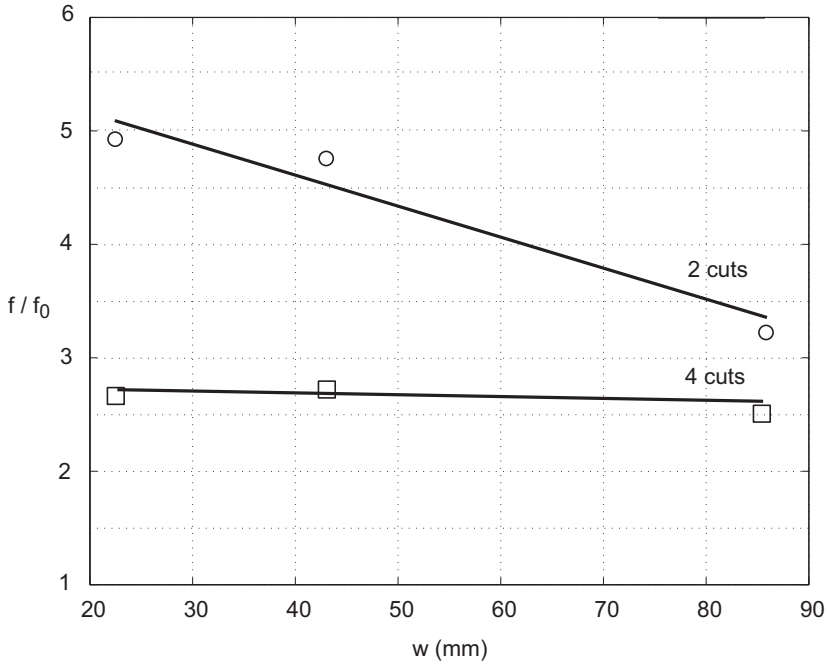

Figure 5: Variation of f with w; f_0 is the fundamental natural frequency of the reflector without skirt.

- increasing the number of cuts decreases f.

Analysis	Cuts	w (mm)	f (Hz)	f/f_0
O1	-	0	$f_o = 5.8$	1
O2			31.5	5.4
E	2	22	28.54	4.9
F	4		15.35	2.7
C	2	43	27.57	4.8
D	4		15.72	2.3
A	2	86	18.62	3.2
B	4		14.46	2.5

Table 2: Natural frequencies in deployed configuration, for $t = 2$ mm.

The second result is slightly counter intuitive. Because f depends on the ratio between modal mass and stiffness, what happens is that the mass penalty associated with increasing the width of the skirt is greater than the increased stiffness provided. Also, if the width of the skirt is increased too much, a low-frequency vibration mode of the skirt alone is observed.

Thus, Figure 5 shows that the largest frequency increase is obtained with the narrower skirt and the smaller number of cuts. In the reflector with four cuts, f is fairly insensitive to the width of the skirt.

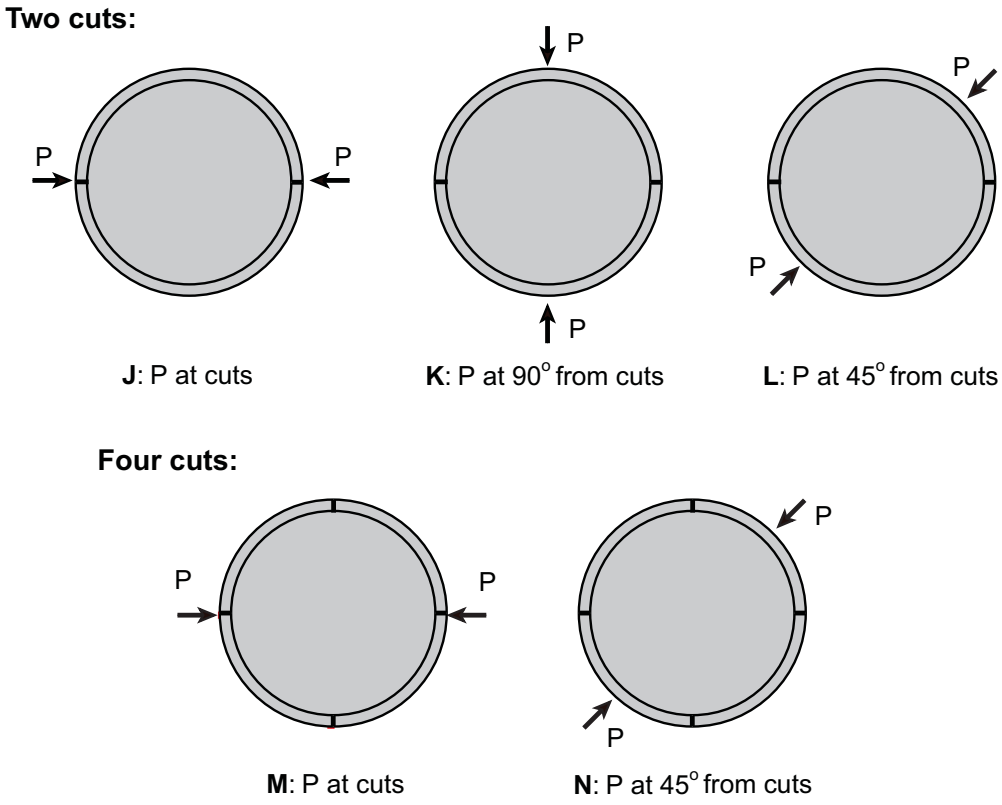

Figure 6: Loading conditions.

Hence, in order to increase the fundamental natural frequency of vibration of the reflector, it is best to use *narrow skirts* and the smallest possible number of cuts.

In conclusion, because the use of the skirt width $w = 22$ mm yields the highest increase in f with the smallest increase in σ_{max}, and because $w = 22$ mm in the small reflector corresponds to $1/20^{\text{th}}$ of the diameter of a general dish; this is a typical value that can be used in future studies.

4.2 Packaging

Further insight can be gained by analysing the force-displacement curve for the reflector under the action of two equal and opposite forces P, whose position with respect to the cuts in the skirt is varied, Figure 7. Note that the displacement plotted here is that of *one* loaded point: the point diametrically opposite moves by an equal amount.

Three different locations of P are considered for the reflector with two cuts, cases J-L, and only two for the reflector with four cuts, cases M-N, see Figure 6. In addition, reflectors without skirt, case O1, and with a continuous skirt, case O2, are considered as reference. The force-displacement curves for these six cases are shown in Figure 7. Note that the skirt width is 22 mm in all cases.

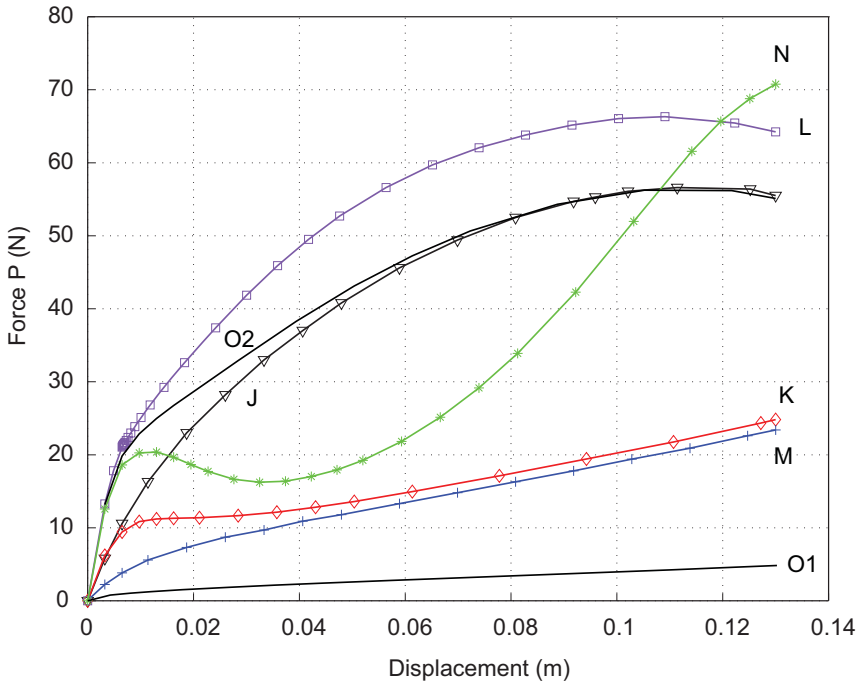

Figure 7: Force-displacement plots for the different loading configurations.

Analysis N, four-cut configuration loaded at 45° from the cuts, is the most interesting as it shows a snapping behaviour after an initial, linear response. The segments of the skirt to which loads are applied snap at $P \approx 20$ N and the deformation of the reflector can be seen in Figure 8. This type of behaviour is very desirable as the dish is "locked" in the fully-deployed configuration until a sufficiently large force is applied to it.

The other curves do not show any snapping, but it is useful to divide the response curves into four sets, as follows.

1. Low initial stiffness and low packaging force. This is obtained for the first reference case —O1, no skirt— and also for case M —skirt with four cuts, loaded at the cuts. The reason for the low packaging force, which is only four times higher than if no skirt is included, is that the reflector folds into two almost rigid half-shells connected by an elastic "hinge" aligned with the two cuts at 90° from the loads. The transverse curvature in this hinge increases with the amount of folding and its longitudinal curvature is approximately zero. Hence, after some initial non-linearity the force displacement relationship is almost linear.

2. High initial stiffness and low packaging force. This is the behaviour for case K —skirt with two cuts, loaded at 90° from the cuts. Although the initial stiffness in this case is more than double the first, due to the smaller number of cuts, for sufficiently large displacements the force-displacement relationship practically coincides with M.

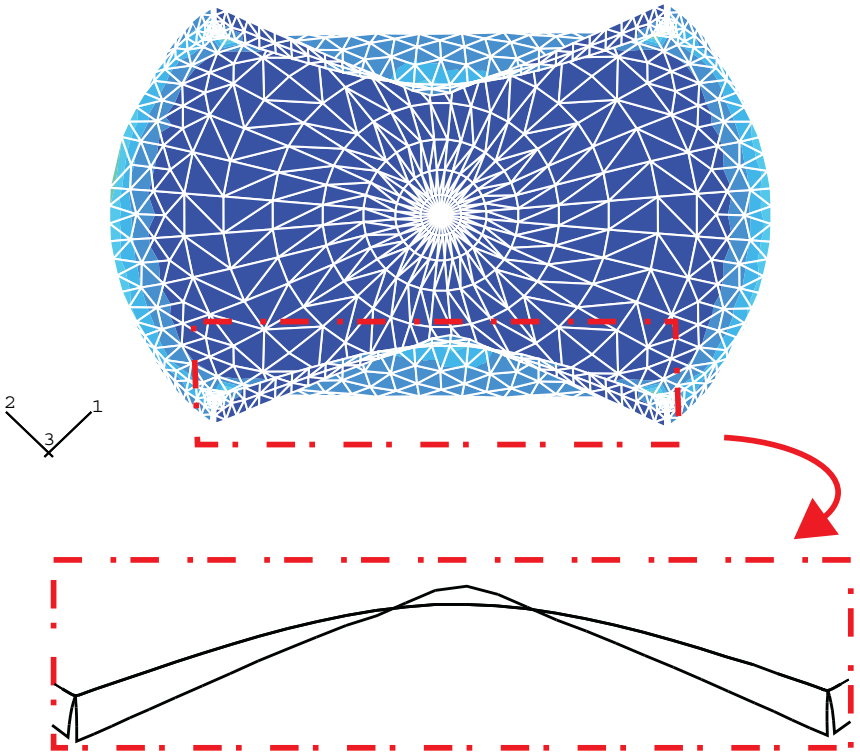

Figure 8: Snapping of skirt in case N.

3. High initial stiffness and high packaging force. This is obtained for case J —only two cuts and P applied at the cuts. The initial stiffness is unchanged from the previous case, but the large displacement regime is much stiffer because it is no longer possible to form an elastic fold aligned with the cuts.

4. Very high initial stiffness and high packaging force. This is the response in case N, already discussed, and L. The initial stiffness matches that of the reflector with continuous skirt, O2, and the forces P required for full packaging are very high. It is surprising that the reflector with the continuous skirt turns out to require a *smaller* packaging force in the end but, in view of the significant amount of skirt deformation that has occurred by this stage, it is clear that any expectation based on linear, small-displacement behaviour, is no longer valid.

4.3 Experimental Verification

In order to gauge the validity of the finite element model, a simple experiment was set up to measure the load-displacement relationship for a polycarbonate shell with diameter of 452 mm, plus the skirt. A schematic of the experimental setup is shown in Figure 9.

Displacement transducers were connected to the points of loading, at the attachment between

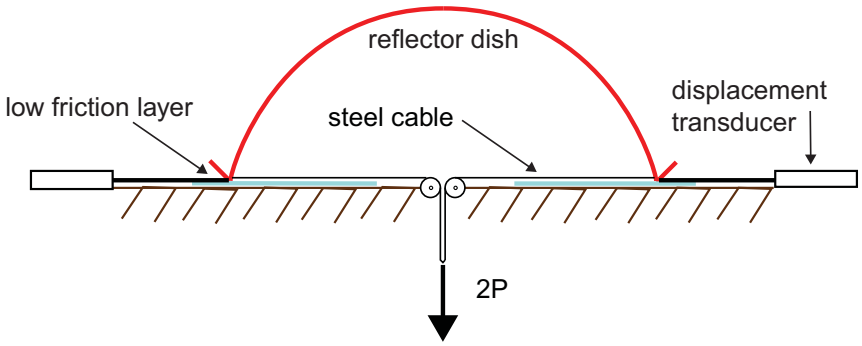

Figure 9: Experimental setup.

the skirt and the rim of the dish. Loads were applied to two diametrically opposite points on the rim using weights hung to a cable and pulley system. This is not an ideal arrangement, and is currently being replaced by a displacement controlled system.

To reduce the stress concentration at the end of the slits, a 3 mm long circumferential slit was formed at end of the radial cut, hence forming a T-shaped cut. At the time of writing, tests have been carried out only on a 1 mm thick dish with a skirt 43 mm wide, loaded at 90° from the cuts.

Figure 10 shows a comparison of the finite-element predictions with three sets of experimental measurements. Note that, as before, the displacement plotted is that of one loaded point. The scatter in the displacements measured below $P = 8$ N suggests that —despite the use of steel guides— there is still considerable friction at the interface between the test rig and the shell. Above $P = 8$ N, the measurements are fairly consistent, but the force-displacement measurements are about 10% higher than the finite-element predictions.

It was found that the cuts on the experimental model were not exactly diametrically opposite and, since it is known from Section 4.2 that applying the loads at 90° to the cuts produces the lowest values of P, it is then clear that if the cuts are not exactly opposite the value of P will be higher.

Taking the above into consideration, it can be concluded that the computational model appears to capture the behaviour of the shell.

5 Full-scale reflector

With the knowledge gained from the analyses presented in Section 4, a computational study of a full scale reflector was carried out. The overall dimensions of the structure are given in Table 3

The aim of this analysis was to investigate a dish that is as close as possible to a real spring-back reflector, and hence the finite-element model is quite complex. General modelling issues were covered in Section 2; more details follow.

It is assumed that the reflector is constructed from 0.152 mm thick triaxial plies of CFRP, hence the thickness of each component is a multiple of this value. This material is isotropic, with

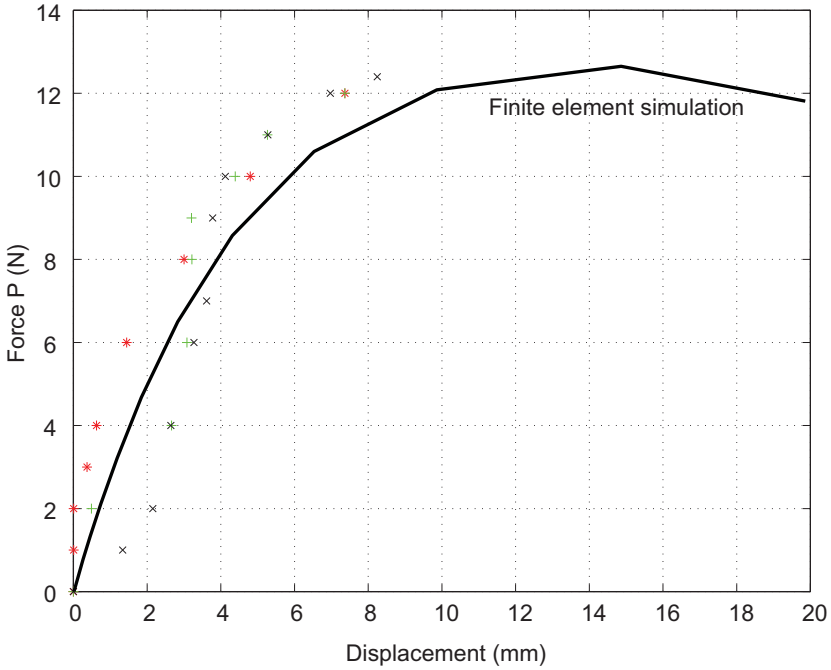

Figure 10: Comparison of three experiments with computational predictions for a polycarbonate dish with two cuts ($w = 43$ mm, loaded at 90° from the cuts).

Young's Modulus of 1.25×10^5 N/mm^2; its Poisson's ratio is taken as 0.3 and the density as 1500 kg/m^3.

Diameter	$D = 5.0$ m
F/D	0.28
Skirt width	$w = 0.125$ m
Skirt angle	100°

Table 3: Dimensions of full-scale reflector.

The thickness of the S3R elements that form the whole reflector is 0.3 mm (2 plies). The 36 radial rib reinforcements are assumed to be 2.43 mm thick (16 plies) and 25.4 mm wide; the triangulation between the radial reinforcements is also 2.43 mm thick and 9 mm wide. The thickness of a circular region of radius 0.83 m at the centre of the reflector has been increased to 1.52 mm (10 plies). The edge reinforcement is 3.2 mm thick (21 plies) and 25.4 mm wide. Skirts of different thicknesses and widths have been considered, but only results for a skirt that is 125 mm wide and 1.52 mm thick (10 plies) are reported.

Before discussing the results for the stiffened reflector, it is useful to know how a dish with the above properties would behave without any stiffening. The maximum Von Mises stress, in the packaged configuration, would be 162 N/mm^2, and the fundamental natural frequency in the

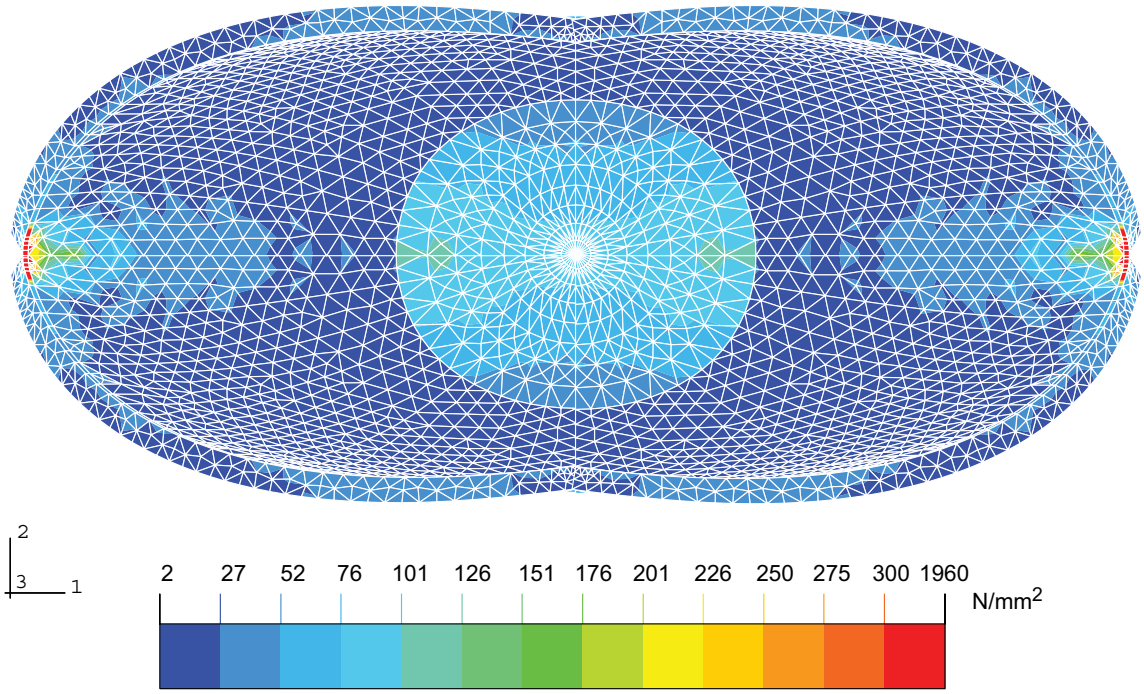

Figure 11: Surface Von Mises stresses in 5.0 m diameter CFRP reflector with four cuts.

deployed configuration 0.64 Hz. The total mass of this reflector is 28 kg. These values provide a reference against which to judge the proposed stiffening system.

5.1 Results

Figure 11 shows the distribution of surface Von Mises stresses in a reflector with four cuts, loaded at two of the cuts, in the packaged configuration. Note that the stresses in the whole of the reflector, apart from two small regions near the cuts in the skirt that open out, are well below 200 N/mm^2. In this small region, shown enlarged in Figure 12, stress levels between 300 and 1960 N/mm^2 are reached both in the edge reinforcement and in two narrow regions that correspond to the joint between the ribs and the associated triangulation (barely visible in the figure). Clearly, these values are not acceptable, but they can reduced by redistributing the stiffness of this part of the reflector. Also note that at the end of each cut there is a 150 mm long circumferential slit. Its purpose is to avoid excessive stress concentrations during folding, by allowing the formation of a sufficiently wide elastic fold across the diameter of the reflector.

If the number of cuts in the stiffening skirt is reduced to two and the loads are applied at 90° to the cuts, the overall stress distribution in the packaged configuration is almost identical to that shown in Figure 11. In particular, the maximum stress is approximately the same. However, for this configuration high stresses, “red” in the scale of Figure 11, develop in the skirt, near the points of application of the loads.

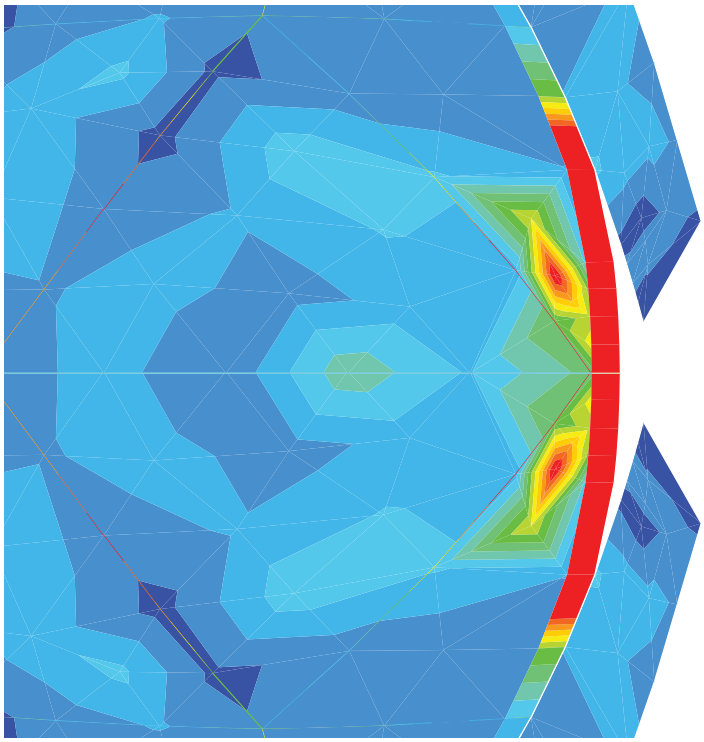

Figure 12: Detail of high stress region in Figure11.

The load-deflection curves for these two stiffened reflectors are compared in Figure 13 to the corresponding curve for the unstiffened reflector. Note that the configuration with two cuts is the only one that shows snapping behaviour: the behaviour of the reflector with four cuts is similar to the unstiffened reflector, although about five times stiffer.

The fundamental natural frequencies of the reflectors with two and four cuts are respectively 1.1 Hz and 4.8 Hz; these values are respectively 1.6 and 7.4 times greater than the frequency of the unstiffened reflector. It is interesting to compare these frequencies to those of a reflector with continuous skirt, 8.6 Hz. This provides an upper bound on the frequency that may be achieved by further improving the design of the stiffening system near the cuts.

6 Discussion

In choosing a stiffening system for spring-back reflectors it is clearly desirable to choose the system that provides the highest stiffness in the deployed configuration, as this will also be the way of best maintaining the surface accuracy of the reflector. The two stiffening systems presented in Section 5 make use of a 125 mm wide skirt, approximately $1/20^{th}$ of the radius of the reflector. These two solutions are equivalent in terms of mass added to the unstiffened reflector, about 16%.

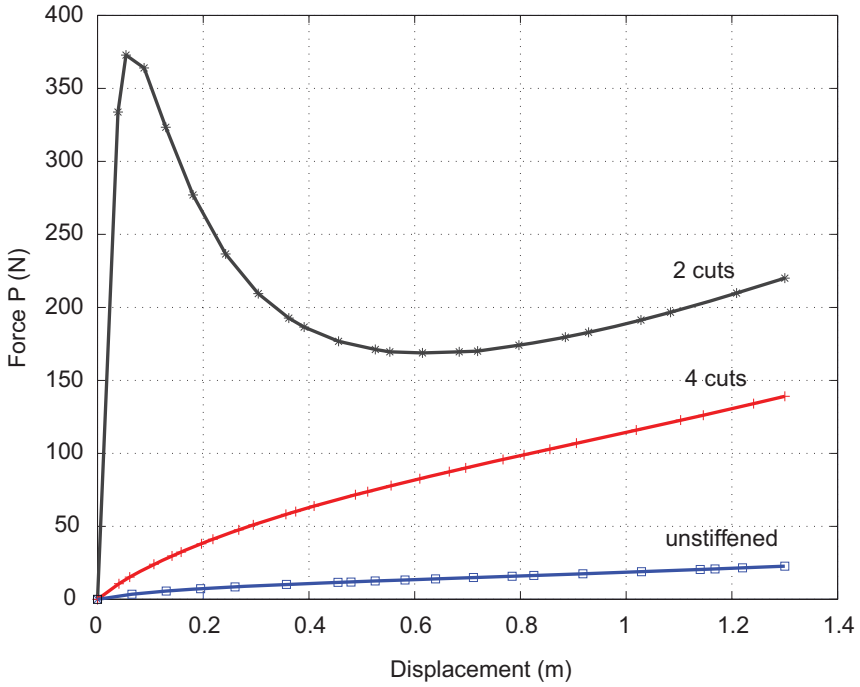

Figure 13: Force displacement relationships for three full-scale reflectors; the two reflectors with cuts are loaded at the cuts.

The skirt with two cuts provides a 20-fold increase in stiffness and a 7.4-fold increase in fundamental natural frequency, but has high stresses in the skirt as well as in the edge reinforcement of the reflector. The skirt with four cuts provides a 5-fold increase in stiffness and 1.6-fold increase in frequency, and has the advantage that the stress levels in the most highly stressed regions can be reduced by relatively minor redesign.

In practice, there are several ways of combining the performance advantages of these two stiffening systems. For example, a way of reducing the stresses in a skirt with two cuts only is to make two additional cuts but join the edges of these cuts with tape springs [6]. Alternatively, a skirt of non-uniform width and thickness may be used to reduce the stress concentrations while maintaining high stiffness.

Finally, note that a skirt width of 125 mm in the full-scale reflector is lower than the value suggested in Section 4.1. This value was chosen to lower the maximum stress, but a problem is that the narrower skirt becomes less effective as soon as two cuts are introduced. This is in contrast with the 22 mm wide skirt considered in Section 4.1 for the small scale model; there the introduction of two cuts decreased f by only about 10%, c.f. analyses O2 and E. Clearly, the linear trends shown in Figure 5 are not valid as $w \to 0$. It is possible, therefore, that an improved design of the stiffening system will yield a natural frequency closer to that of the dish with a continuous skirt.

7 Conclusions

The proposed stiffening method for spring-back reflectors can increase the stiffness of a full-size dish by a factor of 20 and the fundamental natural frequency by a factor of 7.4. The increase in the level of maximum stress during packaging is minimal.

Further improvements on these values will certainly be possible when the detailed design of the skirt is examined more carefully, as suggested in Section 6.

Manufacturing costs for reflectors with the proposed stiffening system are not expected to be significantly higher than for the unstiffened reflector.

References

[1] P. Seizt. *Spar Resolving Spat Over Antenna Work*, Space News, (29 August-4 September, 1994).

[2] Anonymous. *Hughes Graphite Antennas Installed on MSAT-2 Craft*, Space News, (14-20 November, 1994).

[3] G. Greschik, *On the practicality of a family of pop-up reflectors*, 9th Annual AIAA/Utah State University Conference on Small Satellites, 18-21 September 1995.

[4] Hibbitt, Karlsson and Sorenson, *ABAQUS Version 5.8* Hibbitt, Karlsson & Sorenson, 1080 Main Street Pawtucket, Rhode Island 02860-4847 , USA, 1998.

[5] The MacNeal-Schwendler Corporation, *MSC/PATRAN Version 8.5* MSC Software, Los Angeles, California, USA May 1999.

[6] K. A. Seffen and S. Pellegrino, *Deployment dynamics of tape springs*, Proc. Roy. Soc. London, series A 455, (1999), 1003-1048.